Original Article

Glutathione-conjugated sulfanylalkanols are substrates for ABCC11 and γ-glutamyl transferase 1: a potential new pathway for the formation of odorant precursors in the apocrine sweat gland

Tim Baumann[1,2], Sophia Bergmann[1], Thomas Schmidt-Rose[1], Heiner Max[1], Annette Martin[3], Bernd Enthaler[1], Lara Terstegen[1], Dorothea Schweiger[1], Hubert Kalbacher[4], Horst Wenck[1], Gabriele Jedlitschky[2] and Zorica Jovanovic[1]

[1]Research Center, Beiersdorf AG, Hamburg, Germany; [2]Department of Pharmacology, Center of Drug Absorption and Transport, Ernst-Moritz-Arndt-University, Greifswald, Germany; [3]Ansbach University of Applied Sciences, Ansbach, Germany; [4]Medical and Scientific Research Centre, University of Tübingen, Tübingen, Germany

Correspondence: Zorica Jovanovic, PhD, Beiersdorf AG, Unnastraße 48, 20245 Hamburg, Germany, Tel.: +49 40 4909-5446, Fax: +49 40 4909-185446, e-mail: Zorica.Jovanovic@Beiersdorf.com

Abstract: We have previously shown that precursors of odorous components characteristic of axillary sweat are hardly detectable or undetectable in individuals carrying the 538G > A SNP in the *ABCC11* transporter gene. However, it is unclear, whether ABCC11 is directly involved in the transport of these compounds. To approach this question, transport of peptide-conjugated potential precursors of 3-methyl-3-sulfanylhexanol (3M3SH), a key determinant of axillary malodour, was measured using membrane vesicles of Sf9 insect cells overexpressing human ABCC11. Whilst no ABCC11-mediated transport was detected for the dipeptide precursor Cys-Gly-3M3SH, the glutathione conjugate of 3M3SH (SG-3M3SH) was robustly taken up by ABCC11 at a transport rate of 0.47 pmol/mg/min. Collectively, these results illuminate SG-3M3SH as a putative precursor of 3M3SH, which then may undergo intra-vesicular maturation to generate Cys-Gly-3M3SH. Critically, the apocrine sweat gland was demonstrated to express γ-glutamyl transferase 1 (GGT1) protein, which is known to catalyse the deglutamylation of glutathionyl conjugates. Additionally, we provide evidence that recombinant and isolated hepatic human GGT1 is capable of transforming SG-3M3SH to Cys-Gly-3M3SH *in vitro*. To sum up, we demonstrate that the functionality of ABCC11 is likely to play an important role in the generation of axillary malodour. Furthermore, we identify GGT1 as a key enzyme involved in the biosynthesis of Cys-Gly-3M3SH.

Abbreviations: ABCC11, ATP-binding cassette, subfamily C, member 11; 3M3SH, 3-methyl-3-sulfanylhexan-1-ol; cGMP, cyclic guanosine monophosphate; Cys-Gly-3M3SH, 3-(S)-cysteine-glycine-3-methyl-3-sulfanylhexan-1-ol; E(2)17βG, Estradiol-17–β–D–Glucuronide; GGT1, γ-glutamyl transferase; LTC4, leukotriene C4; LTD4, leukotriene D4; SG-3M3SH, 3-(S)-glutathionyl-3-methyl-3-sulfanylhexan-1-ol; TC, Taurocholic acid; DHEAS, Dehydroepiandrosterone sulphate.

Key words: ABCC11 – apocrine sweat – odour precursors

Accepted for publication 11 February 2014

Introduction

The apocrine sweat gland plays the major role in the formation of human axillary odour. However, the physiological function of human apocrine sweat is poorly understood, although in numerous higher mammals, apocrine odour molecules serve as messengers in olfactory communication, for example, to attract mates, to signal danger (fight or flight) and to mark territory (1). Strong axillary malodour in humans is generally perceived as socially offensive in most cultures and is a troublesome problem for the individuals concerned. The clinical term for this condition is osmidrosis.

On a molecular level, the composition of apocrine sweat has been well characterized. Three major chemical classes of molecules have been identified as key constituents of human apocrine sweat: (a) unsaturated or hydroxylated branched fatty acids with 3-hydroxy-3-methyl-hexanoic acid and *(E)*-3-methyl-2-hexenoic acid as the most abundant odorants providing sweat with the typical acidic note; (b) sulfanylalkanols such as 3-methyl-3-sulfanylhexanol (3M3SH) that are relevant descriptors of sweat due to their low odour threshold (2–4); (c) odiferous steroids including

5α-androst-16-en-3-one and 5α-androst-16-en-3-ol the smell of which is described as urine or musk like (5).

Notably, odour molecules are secreted as non-odorous precursors that are metabolized by bacteria on the skin surface. Fatty acids as well as sulfanylalkanols are secreted as non-smelling amino acid conjugates. For example, Cys-Gly-3M3SH is secreted by the apocrine sweat gland and then broken down to 3M3SH by sequential action of bacterial dipeptidase, tpdA and a cysteine β-lyase of *Corynebacterium striatum* (6). Volatile steroids are likely to be generated by bacterial metabolism on steroidal sulphate conjugates, possibly dehydroepiandrosterone sulphate (DHEAS) and androsterone sulphate, which can be detected in human sweat (7–10).

The individual sweat note is a result of the mixture of the various volatile components, and it is believed to be determined by both the apocrine secretion and the specific axillary microflora (11–13). Strikingly, there are not only profound differences in the odour profile between individuals, but intensity of sweat odour can vary markedly depending on ethnicity. Sweat characteristic of Caucasians and Africans is usually perceived as very intense,

247

Experimental Dermatology

whereas sweat emanating from East Asians is mostly very faint with a slight acidic note (14).

Interestingly, it has been known for a long time that the absence of strong body odour in East Asians is associated with an altered cerumen phenotype (15,16). East Asians with dry and white earwax display faint body odour, whereas East Asians with wet and yellow earwax display strong axillary malodour similar to that of the Caucasian and African population. The ceruminous gland involved in the formation of earwax also belongs to the apocrine-type glands (17).

In apocrine secretion, secretory compounds may be derived from the cytoplasm or may be stored before in apical intra-cellular vesicles (17,18). Several previous studies point to a critical role of the ATP-driven efflux transporter ABCC11 in these apocrine secretion processes (19,20). In 2006, Yoshiura et al. (21) showed that a single-nucleotide polymorphism (SNP) in the *ABCC11* gene (538G→A) is causative of the altered cerumen phenotype. This SNP is common in East Asians (80-95%: Caucasians 0-3%) and results in an amino acid change in the first transmembrane domain (180G→R). They also demonstrated that membrane vesicles from cells expressing the SNP (180R) variant showed a low transport activity for the ABCC11 standard substrate cGMP that was similar to that of control vesicles of mock-transfected cells (21). Furthermore, there is evidence that the SNP variant due to lack of N-linked glycosylation readily undergoes ubiquitination and proteasomal degradation (22–24). As a consequence, the transport protein is not sufficiently expressed in the granules of the gland even if there is transport activity of the protein.

We have previously demonstrated that *ABCC11* SNP carriers show diminished quantities or even lack odour precursors that are abundant in the sweat of Caucasians, including Cys-Gly-3M3SH, the precursor of 3M3SH, which is crucial for the typical sweat impression characteristic of Caucasians (14). Functionally, ABCC11 is known to be a transporter for amphiphilic anions and to have a wide substrate spectrum including DHEAS, cyclic guanosine monophosphate (cGMP), estradiol-β-D-glucuronide as well as leukotriene C4 (25,26).

Based on the altered odour bouquet of SNP carriers together with the substrate spectrum of ABCC11, it is perceivable that the function of ABCC11 as a transporter is of critical importance to the generation of axillary malodour. However, it was also observed that the apocrine sweat gland of SNP carriers differs from the wild type in some morphological features (14,18), and morphological differences had also been previously reported between the wet and dry types of ceruminous gland (27,28). Thus, it is unclear so far whether the dysfunction of ABCC11 is directly causative of the odour phenotype in SNP carriers or whether the lack of body odour is a result of developmental effects the mutation might have on the apocrine sweat gland.

Here, we show for the first time that the glutathionyl conjugate of 3M3SH is transported by ABCC11, whereas the Cys-Gly conjugate that can be detected on the skin is not. Moreover, we propose a metabolic model for the generation of Cys-Gly conjugates of 3M3SH in the apocrine sweat gland.

Methods

In vitro ABCC11 transport assay

Transport assays were performed based on the rapid filtration protocol established by Leier et al. (29). ABCC11 and control mem-brane vesicles, respectively (50 μg; Gibco, Darmstadt, Germany), were prepared in buffer containing 50 mM D-mannitol, 50 mM TRIS-Base, pH 7.0, 8 mM K_2CO_3, 10 mM $MgCl_2$, 10 mM phospho-creatine, 4 mM ATP or AMP, 75 mU phosphocreatine kinase and radiolabelled substrate in a total volume of 75 μl. The following ra-diolabelled substrates were used: [estradiol–6,7–^{3}H(N)-17–β–D–glu-curonide, [^{3}H–(G)]taurocholic acid, [14,15,19,20–^{3}H(N)]-leukotriene C_4 and [14,15,19,20–^{3}H(N)]-leukotriene D_4 (all from Perkin Elmer, Waltham, MA, USA) and [8–^{3}H]cyclic guanosine–3′,5′–monophosphate (Hartmann Analytic, Braunschweig, Germany).

Samples were incubated at 37°C, and 20 μl were removed after 5, 30 and 60 s. The transport was stopped by transferring the samples in 1 ml stop solution (50 mM D-mannitol, 50 mM TRIS-Base, pH 7.0). Using vacuum filtration, samples were sucked through 0.22 μm GVWP filters (Millipore, Billerica, MA, USA). Filters were washed five times with 1 ml stop solution and trans-ferred into scintillation vials. Radioactivity was assessed using a liquid scintillation counter. Net ATP-driven transport was deter-mined by subtracting values of the corresponding control sample, containing AMP, from the transport in the presence of ATP.

Data analysis

After Gaussian distribution was confirmed for each time point, the two-tailed t-test for independent parameters was applied. Cal-culations were performed using GraphPad Prism (GraphPad Soft-ware, La Jolla, CA, USA). Graphs were also plotted in GraphPad Prism. The interconnecting lines represent the general trend of the data points.

Chemical synthesis of Cys-Gly-3M3SH and SG-3M3SH

The peptides *Cys-Gly-3M3SH and SG-3M3SH* were synthesized according to the protocol described by Starkenmann et al. (30).

ABCC11 inhibitor testing

Inhibition assays were performed with ABCC11 membrane vesicles as described above using 100 nM [^{3}H]-(S)-glutathionyl-3-methyl-hexanol as a substrate. MK571, an inhibitor of ABCC-type trans-porters (Cayman Chemicals, Ann Arbor, MI, USA), was tested at a final concentration of 10 μM. A control without inhibitor was run simultaneously.

Recombinant expression of GGT1 using the baculoviral expression system

Cell culture

TriEx™-Sf9 cells (Merck, Darmstadt, Germany) were maintained at 27°C in Sf9-Insect-Express Medium (PAA, Pasching, Austria) supplemented with 2% (v/v) foetal bovine serum, 100U/ml peni-cillin and 100 μg/ml streptomycin (Invitrogen, Karlsruhe, Ger-many). For initial transfection, Sf9 cells were incubated in unsupplemented Grace's insect medium (Gibco).

Generation of recombinant baculovirus

Recombinant bacmids containing human γ-glutamyl transferase 1 (GGT1) cDNA or mock cDNA were generated using the Bac–to–Bac® system (Invitrogen). Sf9 cells with a maximal confluency of 50% were transfected with 4 μg bacmid by lipofection employing invitrogen Lipofectamine™ 2000 (Invitrogen) according to the manufacturer's instructions. Medium containing recombinant viruses was collected 5 days after transfection. The generated recombinant viruses were amplified to >10^7 viral particles per ml.

Expression of recombinant GGT1 enzyme

TriEx™-Sf9 cells at a confluency of 70% were infected with the recombinant virus at a multiplicity of infection of 5. Cells were

incubated for 48–72 h, harvested and proteins were extracted using the ProteoJet system (Fermentas, St. Leon-Rot, Germany).

Colorimetric assay for detecting GGT1 activity

The GGT activity assay was performed according to *Szasz* (31, 32) and used 1 mM γ-L-glutamyl-p-nitroanilide (Sigma-Aldrich, Steinheim, Germany) as donor substrate and 20 mM glycylglycine (Sigma-Aldrich) as a glutamyl acceptor. Release of p-nitroaniline was monitored spectrophotometrically at 410 nm (Tecan, Maennedorf, Switzerland).

Transformation of Glutathionyl-3M3SH to Cys-Gly-3M3SH *in vitro*

The GGT1-catalysed transformation of SG-3M3SH to Cys-Gly-3M3SH was performed as described above, with the donor substrate being substituted with 1 mM SG-3M3SH. To catalyse the reaction, native protein extracts of GGT1-transfected TriEX-Sf9 cells containing 100 mU of GGT activity were used. In addition, the same quantities of human GGT1 (Cell Sciences, Canton, MA, USA) and bovine GGT1 (MyBioSource, San Diego, CA, USA) isolates were used. The GGT-Inhibitor GGsTop (Wako, Osaka, Japan) was used at 10 μM.

Analytical determination of the biochemical conversion of Glutathionyl-3M3SH to Cys-Gly-3M3SH

MALDI-TOF-MS analyses were performed by the use of an Autoflex III TOF mass spectrometer (Bruker Daltonics, Bremen, Germany) controlled by the flexControl 3.3 software package (Bruker Daltonics). To detect SG-3M3SH, reaction batches (1 μl each) were mixed with 30 μl α-cyano-4-hydroxycinnamic acid (α-CHCA) matrix (saturated in acetonitrile–deionized water, 50/50, v/v), and mass spectra were recorded in the positive reflector mode. To determine the presence or absence of Cys-Gly-3M3SH, 1,8-bis(dimethylamino)naphthalene (DMAN, 20 mg/ml in ethanol) was used as the matrix choosing a mass range of 220–1000 Da and working in the negative ion mode. Notably, by the use of the DMAN matrix, also called proton sponge, ionization occurs already in the matrix–analyte layer, explaining the analytical term matrix-assisted ionization laser desorption (MAILD) instead of MALDI in this special case.

Axillary punch biopsies and sample preparation

Axillary punch biopsies were derived according to the Declaration of Helsinki Principles from Caucasian volunteers who were informed about the purpose of the study and gave freely written informed consent. The study was approved by the local medical ethics committee on 24 February 2012 (Ethik ÄKHH, Hamburg, Germany, reference no. PV3954, study no. S102531). Axillary skin samples were obtained by standard punch biopsies with a diameter of 6 mm and immediately stored on dry ice. Biopsies were then transferred into liquid nitrogen and stored herein until further processing. Serial sections (8 μm) were obtained using a cryostat (CM3050S, Leica, Wetzlar, Germany), mounted on glass microscope slides (Superfrost, Fisher Scientific, Schwerte, Germany), air-dried and stored at −80°C.

Immunohistochemistry

Serial sections (8 μm) of axillary punch biopsies were air-dried and fixed in acetone for 10 min at −20°C. Sections were incubated with Antibody Dilution Buffer DCS LabLine (DCS, Hamburg, Germany) twice for 20 min to prevent non-specific antibody binding. A polyclonal rabbit GGT1 IgG primary antibody (dilution 1:1000; #ab96466, abcam, Cambridge, UK) was applied to the sections for 1 h at room temperature. Next, sections were incubated for 1 h with fluorescent-labelled donkey secondary antibody Alexa 488 (dilution 1:1000; #A-21206, Invitrogen). Core staining was achieved by incubating sections for 1 min with DAPI (Roche, Mannheim, Germany), diluted 1:1000. Between all applications, sections were washed for 5 min with PBS. Negative controls were obtained by omission of the primary antibody. Fluorescence signals were analysed using a BZ-9000 microscope (Keyence, Neu-Isenburg, Germany).

Results

Glutathionyl-3M3SH but not Cysteinyl-Glycyl-3M3SH is transported by ABCC11

To investigate ABCC11-mediated transport, insect cell vesicles enriched with ABCC11 were used. Control vesicles were tested to account for unspecific transport. Prior to measuring the transport of Cys-Gly-3M3SH, ABCC11-mediated uptake of established substrates was determined. As expected, taurocholic acid, estradiol-β-D-glucuronide and LTC4 were robustly transported by ABCC11 (Figures S1 and S2). Interestingly, LTD4, which has not previously been described as a substrate of ABCC11, was identified to be readily transported by ABCC11 at a transport rate of 16 pmol/mg protein at 45 s. However, LTC4 transport by ABCC11 was more sufficient (Figure S2).

Accumulation of the substrate of interest, Cys-Gly-3M3SH, into ABCC11 vesicles was monitored over 60 s. However, ABCC11-mediated transport could not be detected at any time point (Fig. 1a). Even when measuring the accumulation of Cys-Gly-3M3SH in ABCC11 vesicles after 15 min, no transport could be measured (data not shown).

As glutathione conjugates are well-described substrates of ABCC11 and as LTC4 was found to be transported by ABCC11, too, SG-3M3SH was proposed to be the precursor molecule of Cys-Gly-3M3SH that gets transported by ABCC11. ABCC11-mediated transport of this potential substrate was measured for 60 s. In contrast to the Cys-Gly conjugate, SG-3M3SH was transported by ABCC11 vesicles with an uptake rate of 0.47 pmol/mg/min at 100 nM substrate concentration. No significant accumulation of substrate was measured in control vesicles (Fig. 1b).

The transport of SG-3M3SH by ABCC11 was completely blocked by MK571, a well-established ABCC transporter inhibitor (29), at 10 μM, as measured after 60 s (Fig. 2).

Maturation of Glutathionyl-3M3SH to Cys-Gly-3M3SH mediated by GGT1

Expression of GGT1 in the apocrine sweat gland

Cys-Gly-3M3SH is detectable on the axillary skin surface, whereas SG-3M3SH has not been described as a sweat component (3,6). Therefore, the question arises how and where the glutathionyl conjugate is metabolized to the secreted dipeptide conjugate. A similar conversion step of SG conjugates to Cys-Gly conjugates occurs as part of the mercapturic pathway, a detoxification pathway of the liver and the kidney. Hence, it was hypothesized that the key enzyme catalysing this step, namely γ-glutamyl transferase (GGT), might play a critical role in the deglutamylation of the glutathionyl conjugate of 3M3SH. Indeed, *GGT1* is expressed in the apocrine sweat gland according to microarray data of laser capture microdissected apocrine sweat glands (Agilent Whole Human Genome Oligo Microarrays, Miltenyi Biotec, Bergisch Gladbach, Germany; data not shown).
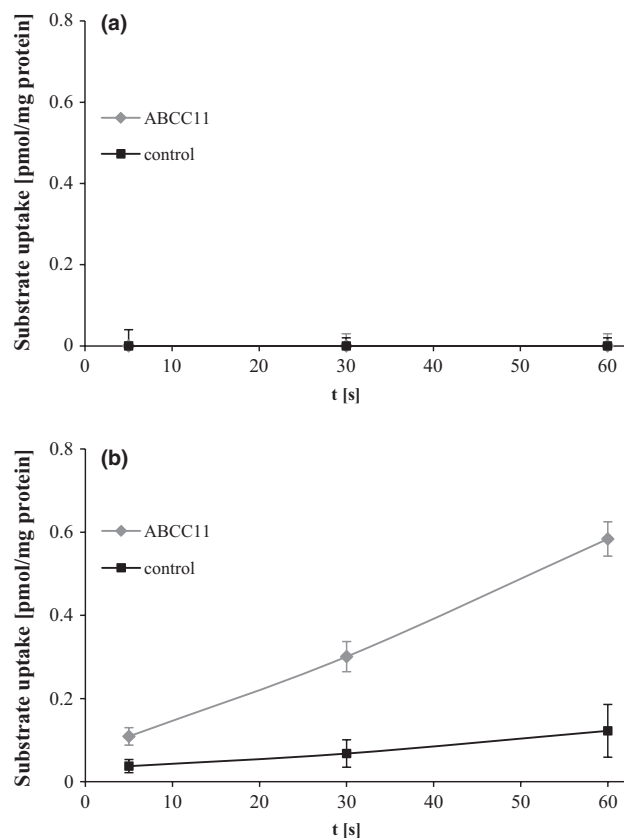
Figure 1. Cys-Gly- (a) and SG-3M3SH (b) uptake by ABCC11 vesicles. Time course of ATP-dependent uptake of [³H]-Cys-Gly-3M3SH (a) and [³H]-SG-3M3SH (b) into membrane vesicles prepared from Sf9 cells transfected with ABCC11 (squares) and control Sf9 cells (cross), respectively. Vesicles were incubated at 37°C in uptake buffer containing 100 nM of substrate. The values shown represent means ± SD; each experiment was performed in triplicates.
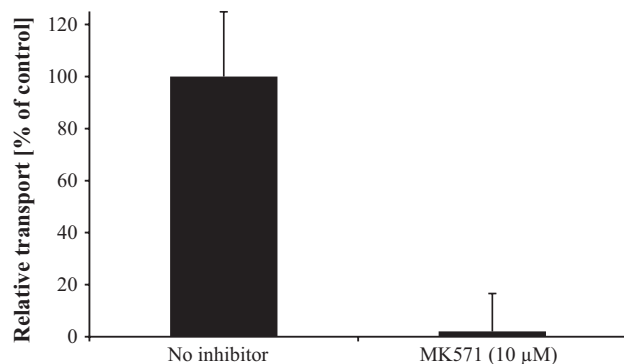

Figure 2. Inhibition of ABCC11-mediated uptake of SG-3M3SH by MK571. Uptake of SG-3M3SH into ABCC11 vesicles was measured in presence and absence (DMSO vehicle control) of the inhibitor MK571 at a concentration of 10 μM. The values represent means ± SD; each experiment was performed in triplicate. The relative transport of the control without inhibitor was set at 100%.

To examine the localization of GGT1 protein in the apocrine sweat gland, immunohistochemistry was applied. On protein level, GGT1 is expressed in the apical part of secretory cells in the apocrine sweat gland. Strikingly, singular secretory cells showed very

strong staining, whereas other secretory cells showed a weak, diffuse GGT1 expression (Fig. 3).

GGT1-mediated transformation of SG-3M3SH to Cys-Gly-3M3SH in vitro

Given that the apocrine sweat gland possesses the enzymatic equipment for the deglutamylation of glutathionyl conjugates, the aim was to examine whether GGT1 is capable of converting SG-3M3SH to Cys-Gly-3M3SH *in vitro*. To this end, SG-3M3SH was incubated with isolated native human GGT1 (sample 1; Table S1), isolated bovine GGT1 (sample 2) and recombinant human GGT1 (sample 5). Alongside *in vitro* control experiments were run without enzyme (sample 3) and with mock lysate (sample 4). To investigate whether biotransformation of SG-3M3SH can be blocked by a GGT1 inhibitor, GGsTop™ was incubated with the reaction mixture containing SG-3M3SH and GGT1 (sample 6). As a positive control for the detection of the expected deglutamylation product, Cys-Gly-3M3SH was included as an additional sample (sample 7). Each reaction batch contained the glutamyl acceptor glycylglycine. After a reaction time of 1 h, each reaction mix was analysed by MALDI-TOF-MS. Relevant mass spectra focusing on the detection of SG-3M3SH and Cys-Gly-3M3SH are provided in Fig. 4.

Figure 4a displays the mass spectrum of sample 1 obtained by MALDI-TOF-MS analysis. Notably, the mass signal for SG-3M3SH was not detected in the sample. However, the mass signal derived from Cys-Gly-3M3SH was robustly detected at m/z 291.17 $[M-H]^-$. Hence, the biotransformation of SG-3M3SH to Cys-Gly-3M3SH catalysed by isolated human GGT1 from liver tissue was confirmed by analytical means. A similar result was obtained when using recombinant human GGT1 (sample 5). In both analyses, the absence of the SG-3M3SH-specific mass signal is indicative of a complete transformation to Cys-Gly-3M3SH under the applied conditions. As demonstrated in Fig. 4b, Cys-Gly-3M3SH was absent in sample 2, containing SG-3M3SH and isolated bovine GGT1. As expected, no Cys-Gly-3M3SH was detected in sample 3 containing SG-3M3SH without enzyme (Fig. 4c). Consistent with that, the mass signal for SG-3M3SH was still present in this sample. This sample is of huge importance to prove the capability of the method and to exclude the detection of potential artifacts
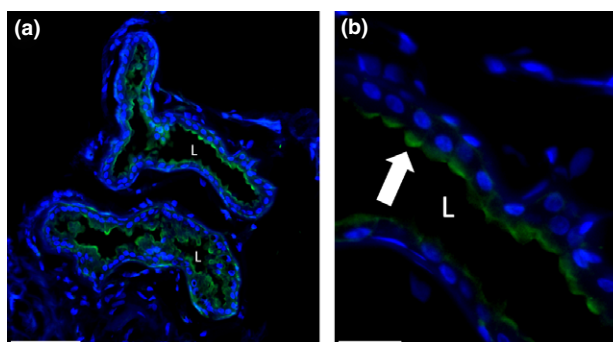

Figure 3. Immunolocalization of γ-glutamyl transferase 1 (GGT1) protein in apocrine sweat glands. (a) Overview of apocrine sweat gland. The GGT1 signal can be detected in secretory cells, but not in myoepithelial cells or the connective tissue of the dermis. Scale bar corresponds to 100 μm. (b) Magnification of the secretory coil. GGT1 signal is restricted to the apical portion of secretory cells (indicated by arrow). Scale bar corresponds to 25 μm. L: lumen; green signal: specific staining of GGT1; blue signal: DAPI staining of the nuclei.
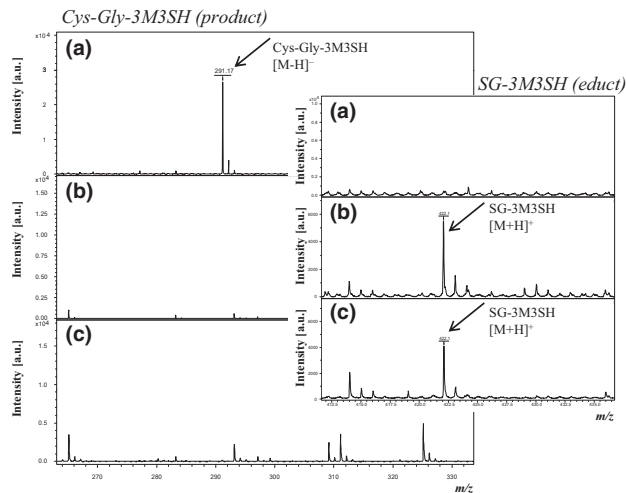
Cys-Gly-3M3SH (product)

SG-3M3SH (educt)

Figure 4. Mass spectra data showing metabolism of SG-3M3SH by human and bovine γ-glutamyl transferase 1 (GGT1). (a) Sample containing SG-3M3SH and human GGT1 shows Cys-Gly3M3SH formation after reaction time. At the same time, SG-3M3SH is not detectable any more. (b) In the reaction batch containing SG-3M3SH and bovine GGT, generation of Cys-Gly-3M3SH cannot be observed. SG-3M3SH detection is unchanged after the reaction time. (c) In the sample containing SG-3M3SH without enzymes, Cys-Gly-3M3SH cannot be detected whereas SG-3M3SH is still present. Displayed details of the mass spectra are focused on the detection of the specific mass signals for Cys-Gly-3M3SH and SG-3M3H (small boxes included in the respective mass spectra). Cys-Gly-3M3SH (m/z 291.17 [M-H]−) was detected in negative ion mode using DMAN as the matrix. The presence of SG-3M3SH was investigated by applying α-CHCA matrix; hence, achieving detection as [M+H]+ adduct (m/z 422.19).

owing to the complexity of the reaction mixtures. Furthermore, in the presence of mock lysate, a transformation of SG-3M3SH was not observed (sample 4, data not shown). The same result was obtained when using 10 μM GGsTop™ inhibitor (sample 6; data not shown). To prove that Cys-Gly-3M3SH (sample 7) can be robustly detected by the applied method, a pure Cys-Gly-3M3SH solution was successfully analysed.

Discussion

To determine whether ABCC11-mediated transport is essential to the formation of body odour on a functional level, we investigated whether the odour precursor of 3M3SH, Cys-Gly-3M3SH, is transported by ABCC11 (6). Even though the concentration of 3M3SH in human sweat is very low, it has got a profound influence on sweat perception due to its low odour threshold (4).

For measuring ABCC11-mediated transport, we used Sf9 insect cell vesicles enriched with recombinant ABCC11 protein. The use of inside-out membrane vesicles from Sf9 cells is a well-established standard method for the characterization of ABC transporter activity (33) as also shown by recent publications, for example, on MDR1 (34) and ABCG2 (35). Adequate human cell systems are not available to date, as it is very difficult to cultivate human axillary cells, especially to a sufficient cell number to prepare membrane vesicles thereof and as no immortalized differentiated secretory cell line from apocrine sweat glands is available.

As numerous sweat constituents are secreted as peptide conjugates, it is of particular interest that the (S)-glutathionyl conjugates leukotriene C4 and (S)-glutathionyl-dinitrophenol were identified to be ABCC11 substrates by Chen et al. As the precursor of 3M3SH, which is detectable on the skin, is a Cys-Gly

conjugate though, we first measured ABCC11-mediated uptake of leukotriene D4, which represents a Cys-Gly conjugate and is a known substrate of ABCC1 (29). Strikingly, leukotriene D4 was identified to be an ABCC11 substrate for the first time. Based on these experimental findings, a transport of the odour precursor of 3M3SH Cys-Gly-3M3SH was likely. However, under the conditions used, an ABCC11-mediated transport could only be detected for the glutathionyl conjugate of 3M3SH, but not for Cys-Gly-3M3SH. Glutathionyl conjugates are well-characterized precursors of Cys-Gly-conjugates present as intermediates in the mercapturic pathway of xenobiotic metabolism in liver and kidney.

Interestingly, apart from ABCC11, a variety of different ABC transporters are well known to be expressed in the skin; for instance, ABCB1 could be detected in eccrine sweat glands (36). Given that ABCC11 is expressed in the apical section of secretory cells of the apocrine sweat gland, it is suggestive of ABCC11 being localized in secretory vesicles that accumulate in this part of the secretory cell. Based on our findings and the location of ABCC11 (14), we postulate that SG-3M3SH is transported into secretory vesicles by ABCC11. As SG-3M3SH cannot be detected on the surface of the skin, we believe that SG-3M3SH undergoes a biotransformation step in apocrine secretory vesicles. Namely, the terminal glutamyl residue gets cleaved off to obtain Cys-Gly-3M3SH. This deglutamylation reaction is typically catalysed by GGTs, which play a key role in detoxification processes (37). Importantly, our microarray data show that GGT1 is an abundantly expressed member of the GGT family in the apocrine sweat gland. The detection of GGT1 protein in the apical part of apocrine secretory cells suggests that ABCC11 and GGT1 are expressed in the same cellular region, which is consistent with our model (Figure S3). In liver and kidney, GGT1 is known to be a membrane-associated ectoenzyme in luminal membranes (38,39). Hence, the natural location of GGT1 at the interface of two compartments supports the idea that GGT1 is an integral part of the membrane of secretory vesicles which in fact represent pseudoextracellular compartments. In addition, our functional data show that human GGT1 is capable of transforming SG-3M3SH to Cys-Gly-3M3SH in vitro. Consequently, our functional data together with the localization support the key role of GGT1 in generating the odour precursor of 3M3SH.

Markedly, GGT1 is well known to transform (S)-glutathionyl conjugates of reactive xenobiotics to Cys-Gly conjugates in the mercapturate pathway of liver and kidney (40). As we demonstrate, it is highly plausible that the function of human GGT1 is essential to the generation of malodour precursors in the apocrine sweat gland, showing the link between detoxification processes and apocrine metabolism. It remains to be shown though whether this reaction can also be catalysed by GGT1 isolated from apocrine sweat glands, as opposed to GGT1 isolates from human liver and recombinant GGT1 as proven above. A singular report on a method for isolating apocrine gland material from axillae has been published by Smythe et al. (41). However, that approach has not been widely used. Most probably this is due to poor availability of appropriate human sample material. Axillary curettage samples from surgical interventions are available, but contain a mixture of different tissues including eccrine sweat glands, connective and adipose tissue.

We identified genes involved in xenobiotic metabolism to be canonically enriched in the human apocrine sweat gland compared

with the eccrine using microarray data (data not shown). Providing the interconnection between xenobiotic pathways and the metabolism of the apocrine sweat gland, the question arises whether the apocrine sweat gland serves as a detoxifying organ.

Human skin is generally accepted to be an excretion organ. Excretion of toxic substances through eccrine sweat is well known and used as a piece of evidence, for example, in drug conviction trials (42). In contrast, the contribution of apocrine sweat to excretion of potentially harmful substances remains elusive. However, it is very unlikely that the apocrine sweat gland plays a relevant role in excretion of toxic or potentially harmful substances given the small secretion volume per day (43). Yet, it is perceivable that the apocrine sweat gland initially served as an excretory organ, using similar metabolic pathways as liver and kidney. This original function might have then changed to a primary role in communication, which a wide body of published data is supporting (44,45). Yet, final evidence as to the physiological role of apocrine sweat is still required.

In summary, we for the first time provide evidence for a metabolic model whereby SG-3M3SH is transported by ABCC11, presumably into secretory vesicles of the apocrine sweat gland, where the terminal glutamyl residue gets cleaved off by the ectoenzyme GGT1. Through this deglutamylation step, Cys-Gly-3M3SH is generated, which ultimately gets onto the skin surface by apocrine secretion. On the skin surface, the odorous mercaptoalkanol 3M3SH is released by bacterial action. However, it is still unclear which metabolite gets processed to obtain SG-3M3SH. Further work is necessary to unravel the metabolic pathways that lead to the generation of axillary malodour.

Hopefully, the identified transport and metabolic processes will help to develop innovative deodorant products that prevent the generation of axillary malodour at its root, providing long-lasting odour control in persons suffering from elevated odour levels.

Acknowledgements

Conflict of interest

The authors have no conflict of interest to declare.

References

1 Albone E S. Scent glands. In: Albone E S, ed. Mammalian Semiochemistry: The Investigation of Chemical Signals Between Mammals. Chichester: John Wiley & Sons Ltd, 1984: 74–134.
2 Hasegawa Y, Yabuki M, Matsukane M. Chem Biodivers 2004: **1**: 2042–2050.
3 Natsch A, Schmid J, Flachsmann F. Chem Biodivers 2004: **1**: 1058–1072.
4 Troccaz M, Starkenmann C, Niclass Y et al. Chem Biodivers 2004: **1**: 1022–1035.
5 Bird S, Gower D B. J Steroid Biochem 1982: **17**: 517–522.
6 Emter R, Natsch A. J Biol Chem 2008: **283**: 20645–20652.
7 Gower D B, Mallet A I, Watkins W J et al. J Steroid Biochem Mol Biol 1997: **63**: 81–89.
8 Labows J N, Preti G, Hoelzle E et al. Steroids 1979: **34**: 249–258.
9 Julesz M. Acta Med Acad Sci Hung 1968: **25**: 273–285.
10 Decreau R A, Marson C M, Smith K E et al. J Steroid Biochem Mol Biol 2003: **87**: 327–336.
11 Natsch A, Gfeller H, Gygax P et al. J Biol Chem 2003: **278**: 5718–5727.
12 Natsch A, Derrer S, Flachsmann F et al. Chem Biodivers 2006: **3**: 1–20.
13 Kuhn F, Natsch A. J R Soc Interface 2009: **6**: 377–392.
14 Martin A, Saathoff M, Kuhn F et al. J Invest Dermatol 2010: **130**: 529–540.
15 Adachi B. Zeitschrift für Rassenkunde 1937: **6**: 273–307.
16 Schiefferdecker P. Zoologica 1922: **72**: 1–154.
17 Gesase A P, Satoh Y. Histol Histopathol 2003: **18**: 597–608.
18 Toyoda Y, Sakurai A, Mitani Y et al. FASEB J 2009: **23**: 2001–2013.

19 Tammur J, Prades C, Arnould I et al. Gene 2001: **273**: 89–96.
20 Bera T K, Lee S, Salvatore G et al. Mol Med 2001: **7**: 509–516.
21 Yoshiura K, Kinoshita A, Ishida T et al. Nat Genet 2006: **38**: 324–330.
22 Toyoda Y, Ishikawa T. Anticancer Agents Med Chem 2010: **10**: 617–624.
23 Nakagawa H, Toyoda Y, Wakabayashi-Nakao K et al. J Pharm Sci 2011: **100**: 3602–3619.
24 Ishikawa T, Toyoda Y, Yoshiura K et al. Front Genet 2012: **3**: 306.
25 Chen Z S, Guo Y, Belinsky M G et al. Mol Pharmacol 2005: **67**: 545–557.
26 Kruh G D, Guo Y, Hopper-Borge E et al. Pflugers Arch 2007: **453**: 675–684.
27 Shugyo Y, Sudo N, Kanai K et al. Am J Anat 1988: **181**: 377–384.
28 Bang Y H, Kim J H, Paik S W et al. Plast Reconstr Surg 1996: **98**: 288–292.
29 Leier I, Jedlitschky G, Buchholz U et al. J Biol Chem 1994: **269**: 27807–27810.
30 Starkenmann C, Niclass Y, Troccaz M et al. Chem Biodivers 2005: **2**: 705–716.
31 Szasz G. Z Klin Chem Klin Biochem 1974: **12**: 228.
32 Szasz G. Clin Chem 1969: **15**: 124–136.
33 Brouwer K L, Keppler D, Hoffmaster K A et al. Clin Pharmacol Ther 2013: **94**: 95–112.
34 Kodan A, Shibata H, Matsumoto T et al. Protein Expr Purif 2009: **66**: 7–14.
35 Ishikawa T, Kasamatsu S, Hagiwara Y et al. Drug Metab Pharmacokinet 2003: **18**: 194–202.
36 Skazik C, Wenzel J, Marquardt Y et al. Exp Dermatol 2011: **20**: 450–452.

37 Stevens J L, Jones D P. The mercapturic acid pathway: biosynthesis, intermediary metabolism, and physiological disposition. In: Dolphin D, Poulson R, Avramovic O, eds. Glutathione Chemical, Biochemical, and Medical Aspects. New York: Wiley, 1989: 45–84.
38 Goldberg D M. CRC Crit Rev Clin Lab Sci 1980: **12**: 1–58.
39 Griffith O W, Bridges R J, Meister A. Proc Natl Acad Sci U S A 1979: **76**: 6319–6322.
40 Habig W H, Pabst M J, Jakoby W B. J Biol Chem 1974: **249**: 7130–7139.
41 Smythe C D, Greenall M, Kealey T. J Invest Dermatol 1998: **111**: 139–148.
42 Genuis S J, Birkholz D, Rodushkin I et al. Arch Environ Contam Toxicol 2011: **61**: 344–357.
43 Wilke K, Martin A, Terstegen L et al. Int J Cosmet Sci 2007: **29**: 169–179.
44 Prehn-Kristensen A, Wiesner C, Bergmann T O et al. PLoS ONE 2009: **4**: e5987.
45 Doty R L, Orndorff M M, Leyden J et al. Behav Biol 1978: **23**: 373–380.

Supporting Information

Additional Supporting Information may be found in the online version of this article:

Figure S1. E(2)17βG and TC uptake by ABCC11 vesicles.

Figure S2. Leukotriene C4 and D4 uptake by ABCC11 vesicles.

Figure S3. Schematic representation of the postulated model for transport and metabolic processes in secretory vesicles of the apocrine sweat gland relevant to the secretion of 3M3SH.

Table S1. Overview of the GGT1 reaction batches with the corresponding MALDI results.